future internet

Article

A Long Short-Term Memory Network-Based Radio Resource Management for 5G Network

Kavitha Rani Balmuri [1], Srinivas Konda [2], Wen-Cheng Lai [3,*], Parameshachari Bidare Divakarachari [4], Kavitha Malali Vishveshwarappa Gowda [5] and Hemalatha Kivudujogappa Lingappa [6]

1 Department of Information Technology, CMR Technical Campus, Hyderabad 501401, Telangana, India; kavitharani.cse@cmrtc.ac.in
2 Department of Computer Science and Engineering (DS), CMR Technical Campus, Hyderabad 501401, Telangana, India; srinivas.cse@cmrtc.ac.in
3 Department of Electronic Engineering, National Yunlin University of Science and Technology, Yunlin 64002, Taiwan
4 Department of TCE, GSSS Institute of Engineering and Technology for Women, Mysuru 570016, Karnataka, India; paramesh@gsss.edu.in
5 Department of Electronics and Communication Engineering, Gopalan College of Engineering and Management, Bengaluru 560048, Karnataka, India; kavishanthagiri@gmail.com
6 Department of ISE, Sri Krishna Institute of Technology, Bengaluru 560090, Karnataka, India; isehod@skit.org.in
* Correspondence: wenlai@yuntech.edu.tw or wenlai@mail.ntust.edu.tw

Abstract: Nowadays, the Long-Term Evolution-Advanced system is widely used to provide 5G communication due to its improved network capacity and less delay during communication. The main issues in the 5G network are insufficient user resources and burst errors, because it creates losses in data transmission. In order to overcome this, an effective Radio Resource Management (RRM) is required to be developed in the 5G network. In this paper, the Long Short-Term Memory (LSTM) network is proposed to develop the radio resource management in the 5G network. The proposed LSTM-RRM is used for assigning an adequate power and bandwidth to the desired user equipment of the network. Moreover, the Grid Search Optimization (GSO) is used for identifying the optimal hyperparameter values for LSTM. In radio resource management, a request queue is used to avoid the unwanted resource allocation in the network. Moreover, the losses during transmission are minimized by using frequency interleaving and guard level insertion. The performance of the LSTM-RRM method has been analyzed in terms of throughput, outage percentage, dual connectivity, User Sum Rate (USR), Threshold Sum Rate (TSR), Outdoor Sum Rate (OSR), threshold guaranteed rate, indoor guaranteed rate, and outdoor guaranteed rate. The indoor guaranteed rate of LSTM-RRM for 1400 m of building distance improved up to 75.38% compared to the existing QOC-RRM.

Keywords: 5G network; burst error; grid search optimization; frequency interleaving; long short-term memory network; Long-Term Evolution-Advanced system; radio resource management

Citation: Balmuri, K.R.; Konda, S.; Lai, W.-C.; Divakarachari, P.B.; Gowda, K.M.V.; Kivudujogappa Lingappa, H. A Long Short-Term Memory Network-Based Radio Resource Management for 5G Network. *Future Internet* **2022**, *14*, 184. https://doi.org/10.3390/fi14060184

Academic Editor: Paolo Bellavista

Received: 4 May 2022
Accepted: 8 June 2022
Published: 14 June 2022

1. Introduction

Modern mobile broadband services are based on the development of the Long-Term Evolution (LTE) and enhanced cellular system. The merits provided by the LTE are low cost per bit, high system capacity, high data rate, and high spectrum efficiency [1,2]. Heterogeneous wireless networks (LTE) are used to satisfy the needs of cellular networks [3,4]. The requirement of broadband mobile traffic is met using the small and macro cells of the heterogeneous networks [5,6]. Device-to-device (D2D) communication is also termed as LTE direct transmission [7]. These D2D communication systems have the capacity to improve the usage of spectral resources and minimize energy consumption. D2D supports peer-to-peer and location-based services and applications [8].

In 3rd generation partnership project LTE, one node is equipped between User Equipment (UE) and enhanced Node B (eNB). The radio network controller in the eNB has the ability to perform traffic balancing, mobility and radio resource management (RRM) [9]. Moreover, the eNB and UE are used to tune the system parameters for achieving an adequate performance, which is defined as self-optimization in LTE [10]. The lesser capability in the cell edge is assumed as the constraint in LTE-Advanced (LTE-A) systems. The interference occurring from the users affects the capacity of the LTE, which causes aggressive frequency. A LTE's random access network is affected because of the complete isolation between different parallel services and signaling overhead [11,12]. The developing characteristics and trends of the 5G LTE-A are cloud radio access network, improved indoor coverage, Human-to-Human and machine-to-machine communications, less delay, less energy consumption, and massive multiple input and multiple output [13].

The development of 5th generation mobile communication networks (5G) satisfies the expected requirements of modern communication, such as huge amounts of connected devices with varying service requirements, high traffic volume, and improved quality of user experience [14]. Therefore, intelligent learning approaches are being developed to improve the performance of the 5G network. Deep learning (DL) is used as a model-free and data-driven approach for minimizing the difficulty with available training inputs and outputs. The issues related to the resource allocation is avoided based on the offline training of simulated data and delivering the results using the well-trained networks during online processes [15]. The interdependency of OSI stack layers is considered to be a key issue in the RRM. An appropriate cross-layer optimization approach is required to obtain an optimal performance for the stack layer. Moreover, access methods with numerous interfaces requires the organization of numerous RRM elements in the same equipment [16]. Examples of the conventional RRM methods are specified as follows: hybrid approach [17], Carrier aggregation-based RRM [18], and pathloss-threshold-based component carrier and cluster configuration algorithm [19]. The main contributions of this paper are as follows:

- An optimal bandwidth and power is assigned to the UEs using the LSTM in the 5G network, whereas the GSO is used to discover adequate hyperparameters.
- An allocation of resources to the unwanted UE is avoided by analyzing the request queue of all the UEs. Additionally, the LSTM-based RRM also reduces the traffic in the network.
- Additionally, a guard level insertion in the data is used to reduce the ISI in the network. The ISI existing in the data creates a high amount of errors during data transmission.

The complete arrangement of the paper is given as follows: Section 2 corresponds to a literature survey covering the existing papers on RRM. Section 3 describes the system model and LSTM-based RRM processed in the 5G environment. The experimental and comparative analysis of the LSTM-based RRM in the 5G environment is given in Section 4. Section 5 provides the conclusions.

2. Literature Survey

Monteiro et al. [20] developed the Distributed RRM (DRRM) for 5G multi-RAT multiconnectivity networks. The wide range of 5G is supported by enabling the tight interworking among the LTE and 5G. The minimum UE throughput is increased by using the optimization problem. This work only achieved less computation effort and less signaling overhead. A higher transmission rate was not achieved when the BS was only considered as the reference signal received power.

Prasad, and Rukmini [21] presented the LTE network over the QoS along with the RRM. The QoS with optimal confederation-aware technology, namely QOC-RRM, was used to allocate the optimum resources for the users in the LTE network. Next, the operators in the LTE network were prioritized by using the recurrent deep neural network. Further, the queuing criterion information was shared by the chaotic weed optimization algorithm to accomplish the routing process that was used for performing data transmission. Then, the

priority of the users for the available resources was scheduled based on the priority value. However, this RRM was analyzed only on fourth generation systems.

Pramudito and Alsusa [22] developed the RRM to enhance the downlink performance of soft-frequency reuse-based LTE. The spectral efficiency of the system is improved by dynamically allocating the RRM in the manner of being distributed and centralized at the network. After performing the allocation, the confederation concept is developed in the network. The confederation style network is combined with a routing algorithm, and this confederation concept is used to minimize the overhead.

Ali et al. [23] developed the predictive RRM (PRRM) scheme for next-generation wireless networks (NGWNs). Additionally, the issues related to mobility management and resource control are addressed while satisfying Quality of Service (QoS) requirements. Therefore, the IEEE 802.21 Media Independent Handover (MIH) protocol is used to optimize the operation among the heterogeneous networks. This MIH protocol delivers the coordination among the two previous network characteristics. Moreover, the PRRM is combined with the handover process, which comprises three phases: resource allocation estimation, radio resource allocation decision, and allocation notification.

Sande et al. [24] presented the Deep Reinforcement Learning (DRL) to perform the RRM in the Integrated Access and Backhaul (IAB) networks. The developed DRL-based RRM is used to mitigate the congestion at the access side of the IAB network. The transmission buffer is initialized to observe the IAB node's congestion rate, which helps to provide the enough resources to the users. Moreover, the dynamic power management and Markov decision process are used to transform the constrained issue due to the problem of power consumption. However, the overall complexity of this developed DRL-based RRM is similar to the existing approach.

Pagin [25] developed the semicentralized resource allocation approach for IAB networks. The developed semicentralized resource allocation is flexible and it has less complexity. Therefore, this flexible semicentralized resource allocation is used to adopt this approach for various needs, cases, and traffic classes of 5G networks. Here, an effective resource allocation is achieved by using generic optimization. However, the developed semicentralized resource allocation is only dependent on the data transmitted and reported in the 3GPP deployment.

Zhao et al. [26] implemented the Reinforcement Learning (RL) for optimizing the dynamic power and performing channel allocation. Here, the Channel State Information (CSI) is combined with the RL for adaptively minimizing the interferences. The interference during the communication is increased according to the number of users.

Giannopoulos et al. [27] developed the power control approach using the Deep Q-Network (DQN) to enhance the system-level Energy Efficiency (EE) of 5G networks [28]. Three different DQN-based approaches, namely centralized, multi-agent, and transfer learning, were developed for confirming the capability of QoS and power-efficient modification in each transmission link. The centralized DQN obtained higher overhead while collecting wide data from the environment.

Sang et al. [29] presented the Predictive Power Allocation (PPA) using Deep Neural Network (DNN) for Vehicle-to-Everything (V2X) communication. The QoS of each route is guaranteed, and the throughput of V2X is increased because of the PPA. The developed DNN-PPA uses the CSI feature of earlier time slots, which does not require any CSI feedback. However, the increment in the transmitted power causes interference.

Hao [30] developed the multi-user Intelligent reflecting surface (IRS)-aided Multiple-Input Multiple-Output (MIMO) system. In IRS-assisted multi-user MIMO, the Base Station (BS), used the chain architecture of sparse RF to minimize circuit power consumption. Here, an Equal Power Allocation Scheme (EPAS) is used to assign the power for all streams on each subcarrier. The weighted sum rate is improved using the joint optimization of the hybrid beamforming in BS. However, inappropriate power allocation to the users of multi-user MIMO affects the performance.

Javornik et al. [31] presented a central-based dynamic RRM algorithm that employs the radio interference maps from local and global Radio Environment Maps (REM), and traffic demands in certain eNB. The radio resources are assigned based on QoS requirements by considering the traffic demands and radio interference maps. Then, the signal strength is calculated by using the REM. This central-based dynamic RRM algorithm is used to mitigate intra- and inter-network interference.

Jacobsen et al. [32] introduced the multi-cell reception technique for improving the capacity of Ultra-Reliable Low-Latency Communications (URLLC) in 5G scenarios, where the multi-cell reception is a joint reception. The integration of multiple Base Stations (BS) is a method from the LTE which is utilized for improving the reliability. Additionally, two multi-cell reception-aware RRM schemes are introduced for allocating the optimal resources to the network, and this developed RRM is depends on the closed-loop power control/modulation and the selection of coding scheme. The substantial gains obtained by the multi-cell reception is less when compared to the single-cell reception.

The disadvantages of existing pieces of research are higher interferences and inappropriate power allocation to the users of the network. In the proposed LSTM-RRM method, the burst errors and ISI are mitigated using frequency interleaving and guard level insertion while broadcasting the data. Subsequently, the LSTM-based RRM is used to allocate an adequate power and bandwidth to the users of the 5G network. Here, the hyperparameter tuning of LSTM is done using grid search optimization.

3. LSTM-RRM Method

The LSTM-based RRM is carried out for allocating the bandwidth and power for the desired UEs. The utilization of LSTM in the 5G environment reduces the complexity during decision making, while hyperparameter tuning is done using GSO. In addition, frequency interleaving is developed in the 5G environment to mitigate the burst errors through the network. Then, guard level insertion is enabled before transmitting the data to minimize the ISI. The block diagram of the LSTM-RRM method is shown in Figure 1.

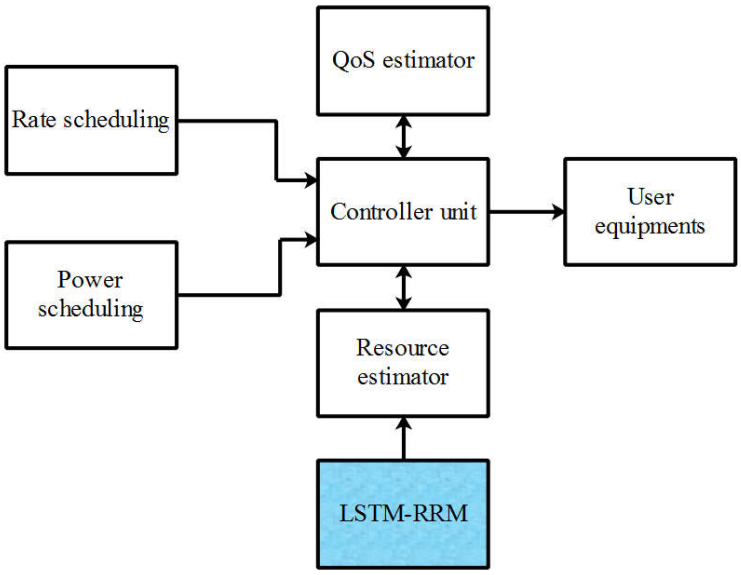

Figure 1. Block diagram of LSTM-RRM method.

3.1. System Model

In a standard LTE, the radio access is mainly dependent on the Single-Carrier Frequency Division Multiple Access (SC-FDMA) and Orthogonal Frequency Division Multiple Access (OFDMA) in uplink and downlink, respectively. The OFDMA and SC-FDMA uses the exact same radio frame structure, which helps to utilize the channel subdivision. Generally, the channels are separated as radio resources which contain domain time and

frequency. The channel bandwidth is varied from 1 to 20 MHz in the frequency domain. Then, the total available bandwidth contains 1.4, 3, 5, 10, 15, and 20 MHz, which are separated into sub-channels of 12 sub-carriers of 15 kHz, totaling 180 kHz. The radio resource's minimum allocation unit is referred to as a Resource Block (RB). Here, the single RB has 1 ms in the time domain and 180 KHz in the frequency domain. The radio resources in the time domain are separated as Transmission Time Intervals (TTI), also referred to as subframes, with 1 ms duration. One frame is created by 10 TTI. Each TTI contains two 0.5 ms slots, and each slot has 7 symbols. In this LSTM-RRM method, the LTE-A considered in the 5G environment is referred to as 5G LTE-A. Here, the system model contains a single cell with one eNB and a set of mobile UEs. The eNB is located in the center with UE, as shown In Figure 2. This 5G LTE-A has two different user traffics: Machine-to-Machine (M-M) and Human-to-Human (H-H) communications. The eNB has a number of resource blocks specified by RBS that are transmitted among the M-M and H-H users.

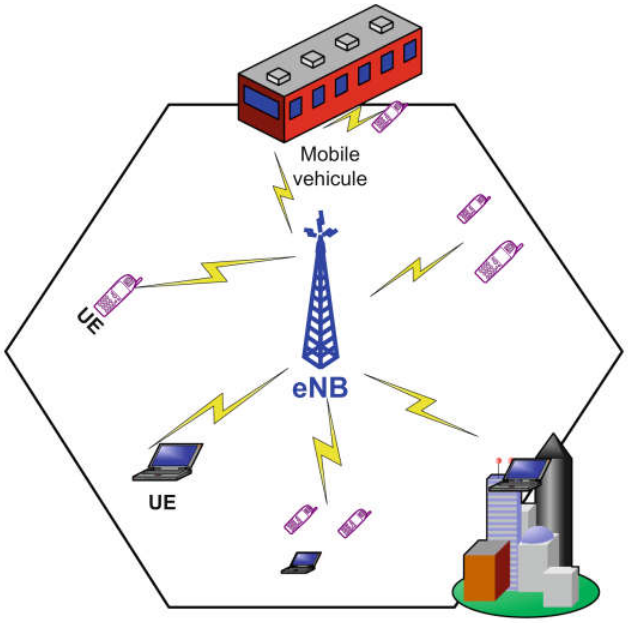

Figure 2. System model.

3.2. Frequency Interleaving and Guard Interval Insertion for Minimizing the Losses through the 5G Environment

When there is continuous data transmission in a single UE with high losses, it creates a burst error through the network. This burst error creates a higher amount of losses during the data transmission. In order to overcome the effects of a burst error, frequency interleaving is developed in the 5G environment. After performing a frequency interleaving, the Inverse Fast Fourier Transform is processed at the transmitter side. Here, the data are transmitted as time domain, not as frequency domain, because the reconstruction of input signal at the receiver side is difficult when the data is transmitted through frequency domain. The input signal transmitted through the time domain is easily reconstructed, even if it is affected by the fading. Subsequently, the signals are converted into parallel to serial. Moreover, the continuous transmission of one by one data causes symbol collision, which produces Inter-Symbol Interference (ISI). This ISI is avoided via guard interval insertion in the parallel-to-serial converted data. After performing this insertion, the data is transmitted using the LTE-A.

In this 5G environment, the Non-Orthogonal Multiple Access (NOMA) is used for obtaining the frequency division multiplexing. The subcarrier provided by the NOMA is used by multiple UEs. Therefore, the NOMA shares the spectrum for two UE with different power in one frequency slot. In addition, the RRM is performed when the network is required to transmit the data for two different UEs in one time slot. The RRM is carried out

based on three different factors: bandwidth, power, and data rate. The 4G network only considers the bandwidth and data rate constraints, it fails to consider the power constraint. However, in this LSTM-RRM method, the power constrains also considered along with bandwidth and data rate constraints to design an effective 5G network. Here, the LSTM is used to perform the efficient RRM over the 5G environment.

3.3. Process of RRM

In LSTM-based RRM, the priority for allocating the resource to the desired UE is identified by analyzing the request queue. Therefore, a UE with high priority is considered as high priority through the network. Before performing the RRM, a set of queues is used to determine which UE the BS receives more request queues from. In this way, the first priority is given to the UE which transmits more queues. The matrixes used in the LSTM are previous values of bandwidth, power, and data rate. Moreover, the hyperparameter tuning of LSTM is performed by using GSO. In RRM, two different resources are allocated based on data rate factors, such as bandwidth and power. The LSTM-based RRM delivers high resources to the UE which has higher requirements in the data transmission. This helps to reduce the amount of request queues transmitted through the network, and it reduces the traffic in the 5G environment. Figure 3 shows the block diagram for the LSTM-based RRM.

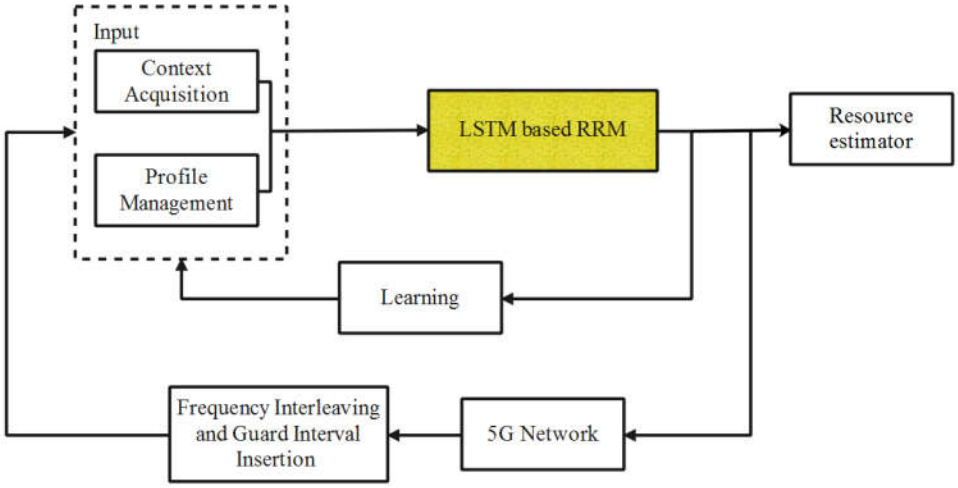

Figure 3. LSTM-based RRM.

This RRM scheme receives the input from two modules (namely context acquisition and profile management) and delivers the output using the LSTM. Here, the RRM is interfaced with the 5G network. The input modules and LSTM used for resource management are described as follows:

- Context Acquisition:

Initially, the context acquisition is used to gather the information of the network components and the UE. Each element of the 5G network uses the monitoring procedure to discover the information. Here, the monitoring procedure provides the information for each component, a certain time period, request queues, and QoS levels. This context information is used to address the problems of the UE that exist in the 5G network.

- Profile management:

The capacities of the segment terminals and elements are provided by the profile management. Moreover, this profile management component also provides the information about the preferences (queues), behavior, constraints, and requirements of the UE. Specifically, this component describes the configurations of the operating parameters, which will be verified for the network elements and terminals. This information is required to perform an appropriate resource management for the UE using LSTM.

- LSTM-based RRM:

The main objective of the LSTM is to exploit all the network resources for obtaining the high amount of bit rates with maximum possible QoS level. Here, the LSTM is used to discover the optimal resource management for serving the UEs with higher QoS level. The detailed description about an effective RRM using LSTM is given in the following section. A clear description about the LSTM-based RRM is given in the Section 3.4.

- Learning:

The learning component of the LSTM has the information about the context acquisition and profile management, where the learning rate of the LSTM obtained from GSO is 0.9. This information helps the LSTM-based RRM scheme to identify and solve the issues.

3.4. LSTM-Based Radio Resource Management

In this 5G network, LSTM is used to accomplish the optimal RRM to improve the bit rate of the communication process. Generally, the LSTM is a special type of Recurrent Neural Network (RNN) that has the capacity for learning long-term dependencies and remembering information for longer periods of time. The LSTM network is arranged in a chain structure, and this LSTM network contains memory blocks, namely cells. In LSTM, two states are moved to the successive cell: cell state and hidden state. Here, the cell state is considered as a key chain of the data flow that allows the data to be transmitted unchanged during the decision-making process. Nevertheless, some linear transformations may occur in the LSTM network. Consequently, the data can be removed from or added to the cell state through the sigmoid gates. The gates of the LSTM are identical to the series or layer of matrix operations that has various individual weights. The long-term dependency problem is avoided by LSTM, due to the utilization of the gates to control the memorization process. The architecture of LSTM is shown in Figure 4.

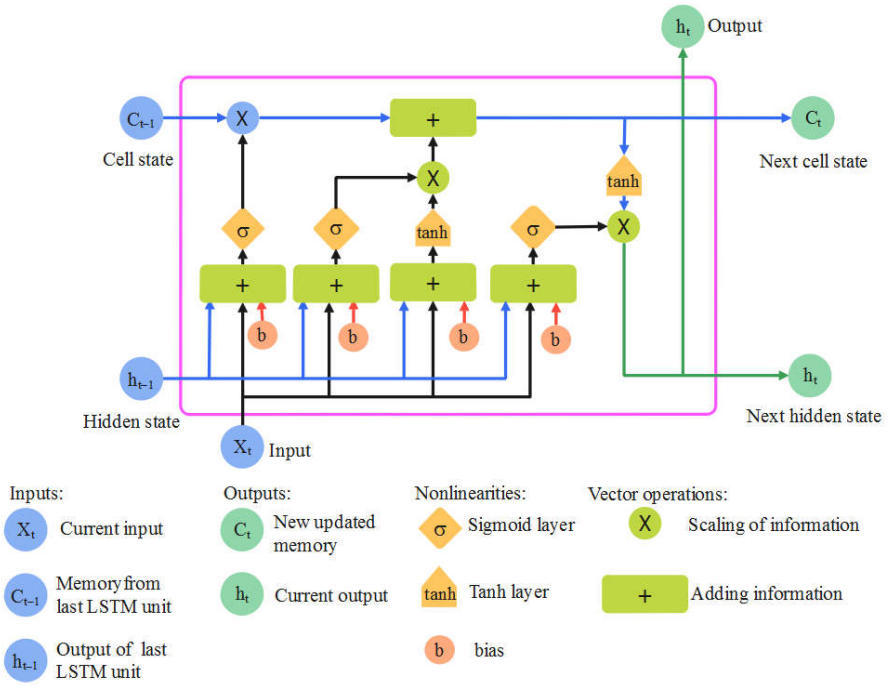

Figure 4. Architecture of LSTM cell.

Initially, the information which is not essential is removed from the cell during the LSTM network construction. The result of the last LSTM unit (h_{t-1}) at time $t-1$ and current input (X_t) at time t are given as input for the sigmoid function. Then, this sigmoid function is used to identify and remove the unwanted data. Moreover, this sigmoid function identifies the part of value which must be removed from the old output. This gate is named

the forget gate (f_t), where the vector value between 0 and 1 is f_t and the respective number of cell states is C_{t-1}.

$$f_t = \sigma\Big(W_f[h_{t-1},\ X_t] + b_f\Big) \tag{1}$$

where the sigmoid function is represented by σ and the weight matrices and bias of forget gate are represented by W_f and b_f, respectively. Moreover, the input X_t considered for this RRM is the data rate value of UEs.

The next step is to choose and save the information of the X_t at cell state as well as its updated cell state. This step has two different parts: sigmoid layer and *tanh* layer. At first, adding or removing the new information is decided using the sigmoid layer, and the value's importance level $(-1\ to\ 1)$ is decided by providing the weight to the values using the *tanh* layer. The new cell state is updated by multiplying the aforementioned values. The input gate output and updated cell state are represented in Equations (2) and (3), respectively. Next, the new memory is included in the old memory C_{t-1}, which results in C_t, as shown in Equation (4).

$$i_t = \sigma(W_i[h_{t-1}, X_t\ ] + b_i) \tag{2}$$

$$N_t = tanh(W_n[h_{t-1}, X_t\ ] + b_n) \tag{3}$$

$$C_t = C_{t-1}f_t + N_t i_t \tag{4}$$

where the cell states at time t and $t-1$ are C_t and C_{t-1}, respectively, and the weight matrices and bias of the cell state are represented as W and b, respectively.

Finally, the output value (h_t) is mainly dependent on the output cell state (O_t). Here, the sigmoid layer chooses which cell is required to deliver the output. Subsequently, the value generated in the cell state (C_t) using the *tanh* layer is multiplied with the result of the sigmoid gate (O_t), which results in a value between -1 and 1. The sigmoid gate and cell output are represented in Equations (5) and (6), respectively.

$$O_t = \sigma(W_o[h_{t-1}, X_t\ ] + b_o) \tag{5}$$

$$h_t = O_t \tanh(C_t) \tag{6}$$

where the weight matrices and bias of the output gate are denoted as W_o and b_o, respectively.

GSO-Based Hyperparameter Tuning for LSTM

In this phase, the GSO [33] is used for optimizing the hyperparameters of the LSTM. The set of hyperparameters processed under hyperparameter tuning are the amount of neurons, learning rate, regression rate (reg_rate), size of batch, and epochs, as given in Table 1. This GSO is used to obtain optimal results when the hyperparameters are not significant. The values given in Table 1 are the range of values in the search space, and the hyperparameter tuning is done according to the power and bandwidth. Here, GSO with 10-fold cross-validation is performed to select the optimal value within the given range of hyperparameters.

Table 1. Parameters of LSTM.

Parameters	Range of Values
epochs	1–200
Neurons	10–200
reg_rate	0.01, 0.05, 0.1, 0.2, 0.3, 0.4, 0.5
learning rate	0.1–0.9
batch_size	73, 146, 219, 500, 1000

Therefore, this LSTM network is trained using the bandwidth, power, and data rate of the UE in the 5G network. The number of data used to train the LSTM is 3628800, which are taken from the simulation when the 5G network is operated without LSTM.

Accordingly, the UEs with higher QoS level are maintained by allocating an adequate power and bandwidth using the LSTM. Consequently, the bit rate of the 5G network is increased during the communication process.

4. Result and Discussion

The results and discussion of the LSTM-RRM method are clearly described in this section. The implementation and simulation of the LSTM-RRM method was carried out in Network Simulator-3, which runs on a Windows 8 operating system with Intel core i3 processor and 4GB RAM. In this LSTM-RRM method, losses in the 5G environment are minimized by using frequency interleaving and guard interval insertion. Subsequently, the LSTM-based RRM is accomplished to allocate adequate resources for the desired UEs. The height of the BS considered for this LSTM-RRM method is 10 m, and the system bandwidth is 100 MHz. The specifications considered for the LSTM-RRM method are shown in Table 2.

Table 2. Specification parameters.

Parameter	Value
Height of BS	10 m
Transmission power of BS	35 dBm
Type of transmission antenna	Narrow beam
System bandwidth	100 MHz
Carrier frequency	28 GHz

4.1. Performance Comparison between LSTM-RRM and DRRM

Here, the performance of the LSTM-RRM method is analyzed in terms of throughput, outage, Jain's index, and dual connectivity. These performances are compared with DRRM [20] to show the effectiveness of the LSTM-RRM method. The DRRM [20] was also implemented and simulated in NS-3 to evaluate the LSTM-RRM method.

Figure 5 and Table 3 show the comparison of UE throughput between DRRM [20] and LSTM-RRM. Here, the comparison is made by varying the number of UEs from 5 to 30. From the analysis, it is concluded that the LSTM-RRM achieves higher UE throughput than the DRRM [20]. For example, the UE throughput of the LSTM-RRM varies from 15 Mbps to 63 Mbps, whilst DRRM's [20] UE throughput varies from 10 Mbps to 61 Mbps. Specifically, the UE throughput of LSTM-RRM for 30 UE is improved up to 50% when compared to the DRRM [20]. The LSTM-RRM achieves higher UE throughput because it mitigates the burst errors by using frequency interleaving, and ISI is minimized by using guard level insertion.

Table 3. Analysis of UE throughput for LSTM-RRM and DRRM.

Number of UEs	UE Throughput (Mbps)	
	DRRM [20]	LSTM-RRM
5	61	63
10	39	44
15	30	35
20	22	28
25	18	24
30	10	15

The comparison of 50 percentile UE throughput between DRRM [20] and LSTM-RRM is shown in Figure 6 and Table 4. Here, the 50th percentile UE throughput is analyzed by varying the UE from 5 to 30. From the analysis, it is can be seen that the 50 percentile UE throughput of LSTM-RRM is higher than the DRRM [20]. For the instance, the 50 percentile UE throughput of LSTM-RRM is in the range from 65 Mbps to 125 Mbps, whereas the DRRM [20] is in the range from 40 Mbps to 95 Mbps. an effective resource allocation over the 5G network is used to increase the throughput of the LSTM-RRM. The 50 percentile

UE throughput of LSTM-RRM for 30 UE is improved up to 62.5% when compared to the DRRM [20].

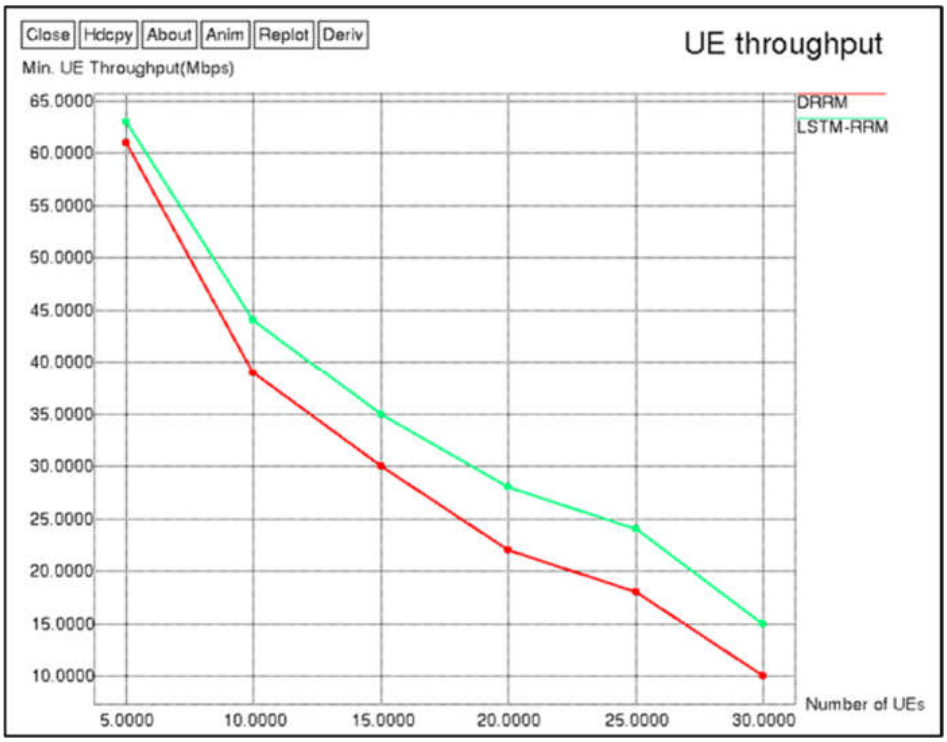

Figure 5. Comparison of minimum UE throughput.

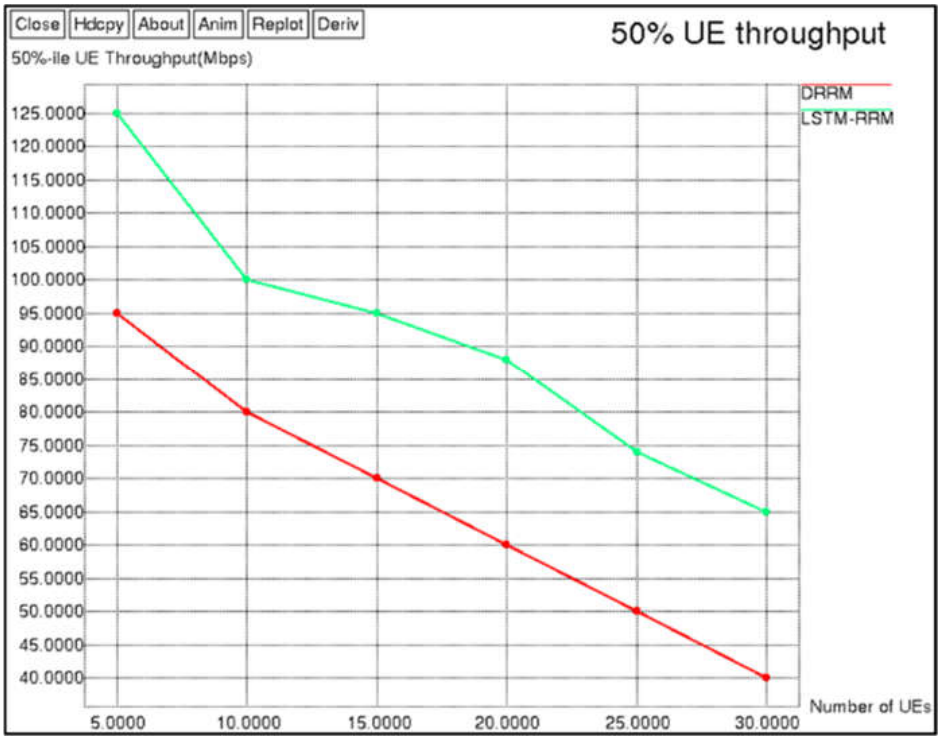

Figure 6. Comparison of 50% UE throughput.

Table 4. Analysis of 50% UE throughput for LSTM-RRM and DRRM.

Number of UEs	50% UE Throughput (Mbps)	
	DRRM [20]	LSTM-RRM
5	95	125
10	80	100
15	70	95
20	60	88
25	50	74
30	40	65

The throughput comparison of 90% UE is shown in Figure 7 and Table 5. Here, the variation of the throughput is analyzed for different numbers of user equipment: 5, 10, 15, 20, 25, and 30. From Figure 7 and Table 5, it can be seen that the LSTM-RRM method obtains higher throughput than the DRRM [20]. For example, the 90% UE throughput of the LSTM-RRM varies from 140 Mbps to 235 Mbps, whilst DRRM [20]'s UE throughput varies from 80 Mbps to 215 Mbps. Specifically, the 90% UE throughput of LSTM-RRM for 30 UE is improved up to 75% when compared to the DRRM [20]. The LSTM-RRM method obtains higher throughput due to the optimal power and bandwidth allocation to the desired UE. Moreover, the losses through the 5G environment are minimized by using frequency interleaving and guard interval insertion. Therefore, the amount of packets received by the BS is increased during the communication.

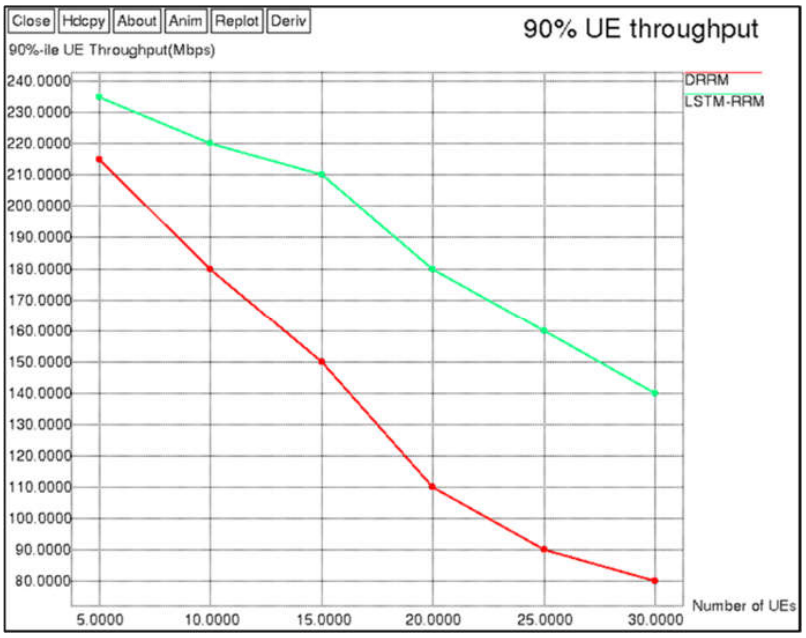

Figure 7. Comparison of 90% UE throughput.

Table 5. Analysis of 90% UE throughput for LSTM-RRM and DRRM.

Number of UEs	90% UE Throughput (Mbps)	
	DRRM [20]	LSTM-RRM
5	215	235
10	180	220
15	150	210
20	110	180
25	90	160
30	80	140

The comparison of outage percentage between the LSTM-RRM method and DRRM [20] is shown in Figure 8 and Table 6, determined by varying the UE from the 5 to 30. This outage analysis shows that the LSTM-RRM method achieves higher outage than the existing DRRM [20]. For example, the outage percentage of LSTM-RRM varies from 87% to 98%, whereas the outage percentage of DRRM [20] varies from 83% to 96%. The outage of the DRRM [20] is less than the LSTM-RRM method due to its complexity. However, the optimal resource allocation of the LSTM-RRM method leads to an increase in outage through the 5G system.

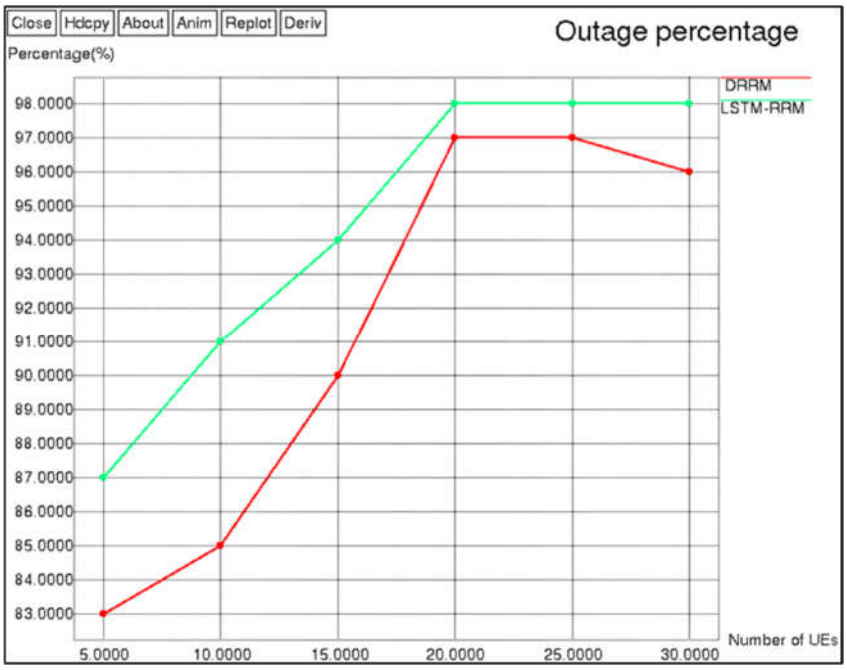

Figure 8. Comparison of outage percentage.

Table 6. Analysis of outage percentage for LSTM-RRM and DRRM.

Number of UEs	Outage Percentage (%)	
	DRRM [20]	LSTM-RRM
5	83	87
10	85	91
15	90	94
20	97	98
25	97	98
30	96	98

Figure 9 and Table 7 show the dual connectivity comparison between the LSTM-RRM method and DRRM [20]. Dual Connectivity (DC) specifies the capacity of connecting the different BSs in the same radio access technology. Specifically, Figure 9 and Table 7 illustrate the percentage of connected UE in dual connectivity with respect to the amount of UEs in the system. The LSTM-RRM method has higher dual connectivity than the DRRM [20] because of its effective RRM between the UEs. The dual connectivity of LSTM-RRM for 30 UE is improved up to 12% when compared to the DRRM [20]. The optimal power and bandwidth allocation using LSTM is used to improve the connectivity in the 5G system.

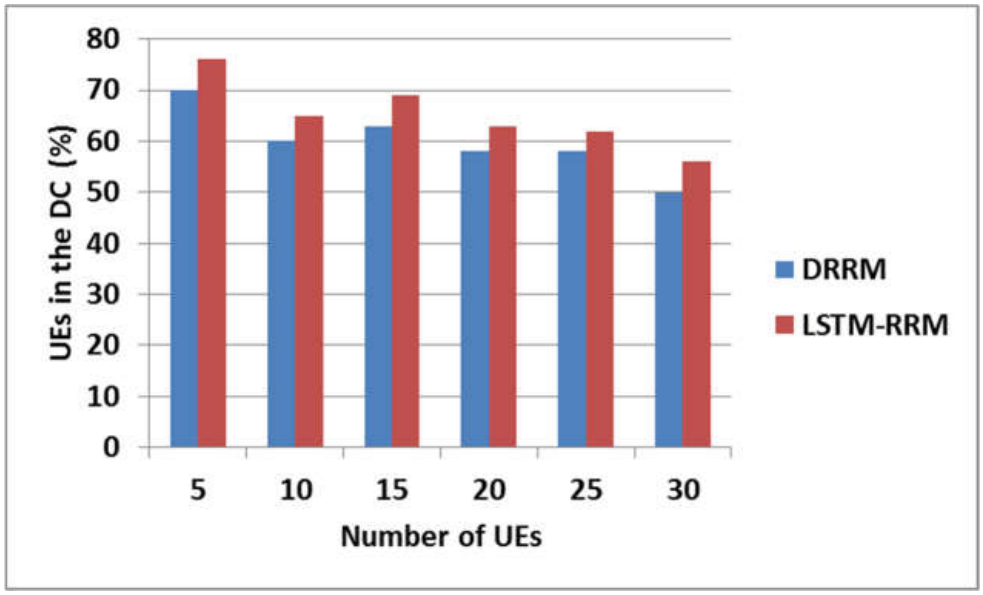

Figure 9. Comparison of dual connectivity.

Table 7. Analysis of dual connectivity for LSTM-RRM and DRRM.

Number of UE	Dual Connectivity (%)	
	DRRM [20]	LSTM-RRM
5	70	76
10	60	65
15	63	69
20	58	63
25	58	62
30	50	56

4.2. Performance Comparison between LSTM-RRM and QOC-RRM

Here, the performance of the LSTM-RRM is analyzed with the QOC-RRM [21] in terms of different QOS parameters such as sum rate, threshold guaranteed rate, indoor guaranteed rate, and outdoor guaranteed rate. The aforementioned performances are analyzed by varying the number of users and distance in the 5G environment. This performance comparison for QOS parameters is described as follows:

The analysis of USR for the LSTM-RRM for 3 Base Stations (BSs) and 20 BSs is shown in Figure 10 and Table 8. Here, the USR is analyzed by varying the users from 10 to 30. From the analysis, it is identified that the LSTM-RRM with the 3 BSs achieves higher USR than the LSTM-RRM with 20 BSs. For example, the LSTM-RRM with 3 BSs achieves USR in the range from 32 Mbps to 91 Mbps, whereas the LSTM-RRM with 20 BSs achieves USR in the range from 22 Mbps to 85 Mbps. The LSTM-RRM with 3 BSs provides significant improvement in USR due to less traffic. The comparison of USR between the LSTM-RRM with EPAS [30] is given in Table 9. Here, the EPAS [30] is taken for comparison because this EPAS [30] also used to allocate the power to the multiple users while broadcasting the data. From the comparison, it can be seen that the proposed LSTM-RRM achieves higher USR than the EPAS [30] due to its optimal power allocation according to the bandwidth, power, and data rate.

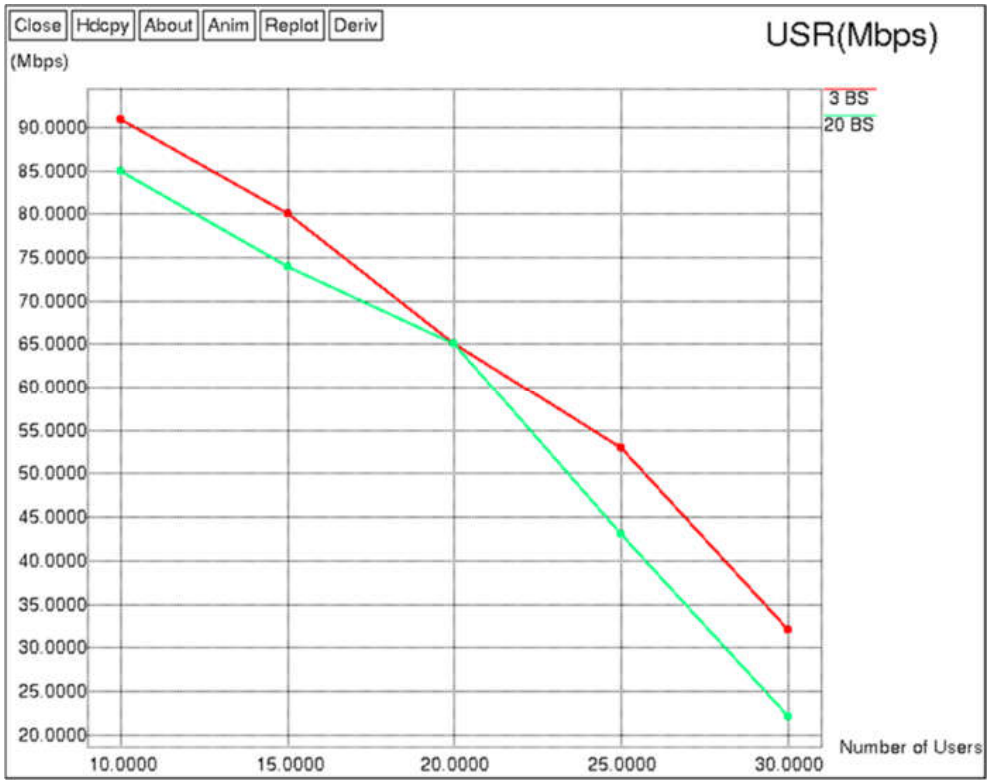

Figure 10. Comparison of USR.

Table 8. Analysis of USR for LSTM-RRM.

Number of Users	USR (Mbps)	
	3 BS	20 BS
10	91	85
15	80	74
20	65	65
25	53	43
30	32	22

Table 9. Comparison of USR for LSTM-RRM.

Number of Users	USR (Mbps)	
	EPAS [30]	LSTM-RRM
15	8.3×10^{-6}	77
20	8.75×10^{-6}	65
25	9.5×10^{-6}	48
30	10×10^{-6}	27

Figure 11 and Table 10 show the TSR comparison between LSTM-RRM with 3 BS and with 20 BS. Here, the comparison is made by varying the number of users from 10 to 30. From the analysis, it can be seen that the LSTM-RRM with 3 BS achieves higher TSR than the LSTM-RRM with 20 BS. For example, the TSR of the LSTM-RRM with 3 BS varies from 31 Mbps to 89 Mbps, whilst the TSR of the LSTM-RRM with 20 BS varies from 23 Mbps to 83 Mbps. Similar to the USR analysis, the LSTM-RRM with 3 BS achieves higher TSR due to less traffic.

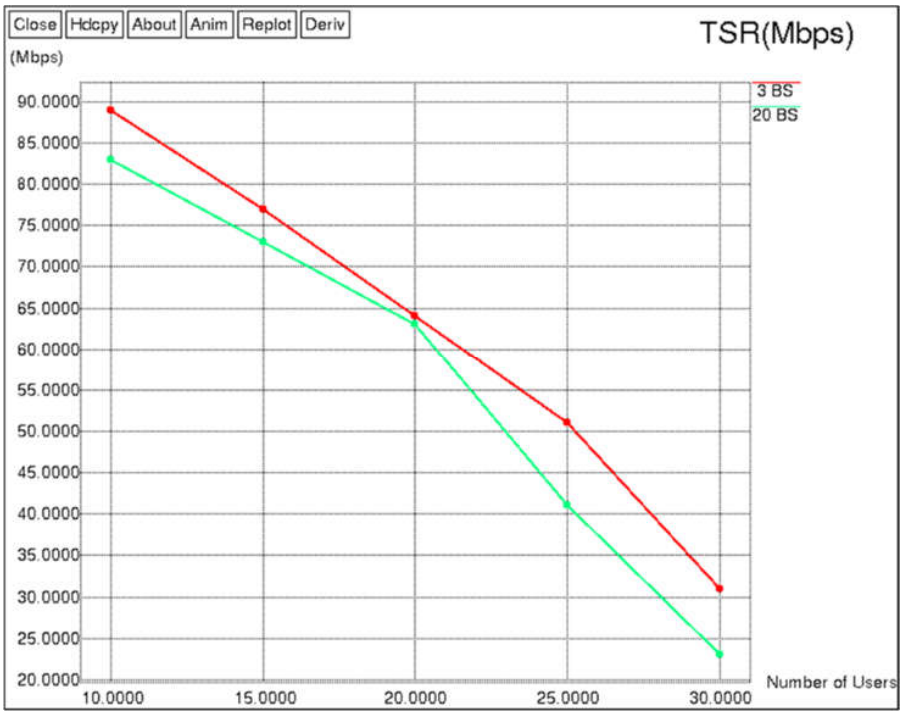

Figure 11. Comparison of TSR.

Table 10. Analysis of TSR for LSTM-RRM.

Number of Users	TSR (Mbps)	
	3 BS	20 BS
10	89	83
15	77	73
20	64	63
25	51	41
30	31	23

The comparison of OSR between the LSTM-RRM and QOC-RRM [21] is shown in Figure 12 and Table 11. Here, the OSR is analyzed by varying the building distance from 400 to 1400. From the analysis, it can be seen that the LSTM-RRM achieves higher OSR than the QOC-RRM [21]. For example, the LSTM-RRM achieves OSR in the range from 25 Mbps to 35 Mbps, whereas the QOC-RRM [21] achieves OSR in the range from 15 Mbps to 25 Mbps. Specifically, the OSR of LSTM-RRM for building distance of 1400 m is improved up to 66.67% when compared to the QOC-RRM [21]. The OSR of LSTM-RRM is increased in the 5G network because of an LSTM-based resource allocation to the required users. Moreover, the interferences and errors are also avoided in the LSTM-RRM by using guard level insertion and frequency interleaving in the 5G network.

Table 11. Analysis of OSR for LSTM-RRM and QOC-RRM.

Building Distance (m)	OSR (Mbps)	
	QOC-RRM [21]	LSTM-RRM
400	25	35
600	23	33
800	21	31
1000	19	29
1200	17	27
1400	15	25

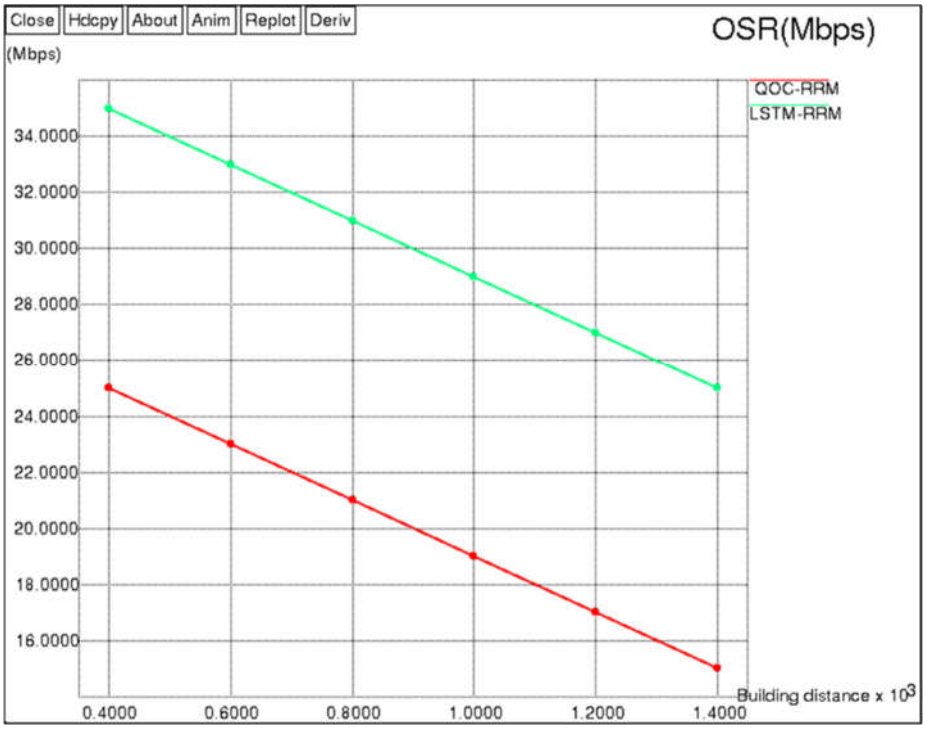

Figure 12. Comparison of OSR.

Figure 13 and Table 12 show the guaranteed capacity comparison between LSTM-RRM with 4 BS and with 15 BS. Here, the comparison is made by varying the threshold from 10 to 30. From the analysis, it can be seen that the LSTM-RRM with 4 BS achieves higher guaranteed capacity than the LSTM-RRM with 15 BS. For example, the guaranteed capacity of the LSTM-RRM with 4 BS varies from 550 kbps to 835 kbps, whereas the guaranteed capacity of the LSTM-RRM with 15 BS varies from 280 kbps to 600 kbps.

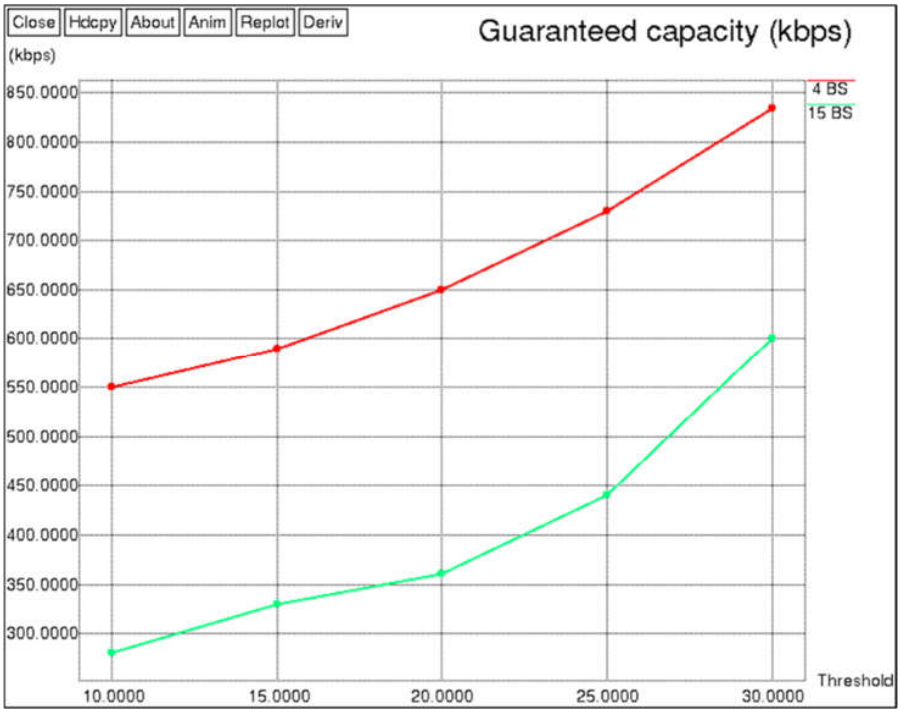

Figure 13. Comparison of guaranteed capacity.

Table 12. Analysis of guaranteed capacity for LSTM-RRM.

Threshold	Guaranteed Capacity (kbps)	
	4 BS	15 BS
10	550	280
15	590	330
20	650	360
25	730	440
30	835	600

The comparison of indoor guaranteed rate between LSTM-RRM and QOC-RRM [21] is shown in Figure 14 and Table 13. Here, the indoor guaranteed rate is analyzed by varying the building distance from 400 m to 1400 m. From the analysis, it can be seen that the LSTM-RRM achieves a higher indoor guaranteed rate than the QOC-RRM [21]. For example, the LSTM-RRM achieves an indoor guaranteed rate in the range from 178 Mbps to 228 Mbps, whereas the QOC-RRM [21] achieves an indoor guaranteed rate in the range from 85 Mbps to 130 Mbps. The indoor guaranteed bitrate of LSTM-RRM for a building distance of 1400 m is improved up to 75.38% when compared to the QOC-RRM [21]. The indoor guaranteed rate of LSTM-RRM is increased by reducing the interferences occurring during the communication.

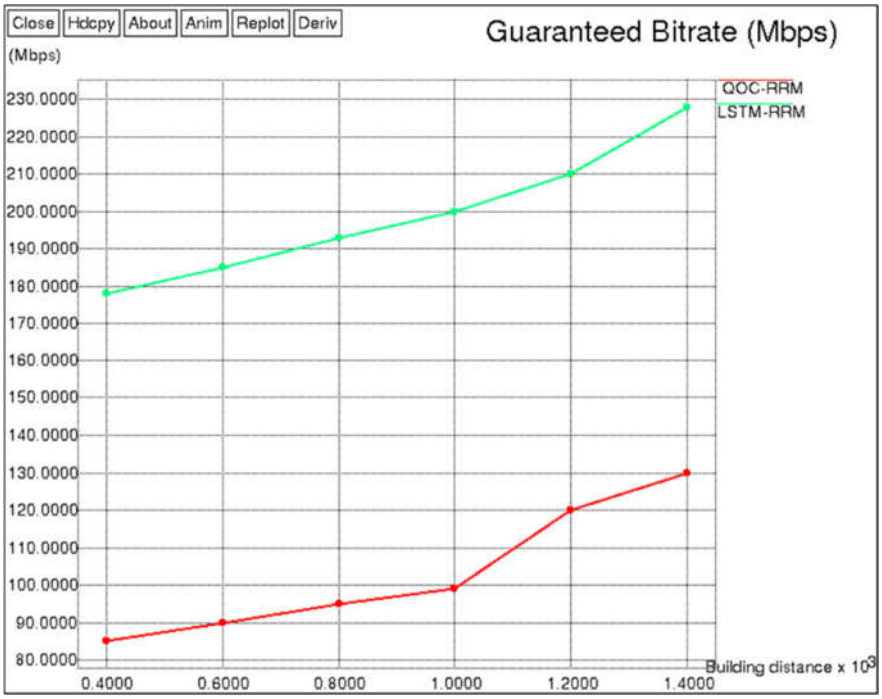

Figure 14. Comparison of indoor guaranteed rate.

Table 13. Analysis of indoor guaranteed rate for LSTM-RRM and QOC-RRM.

Building Distance (m)	Indoor Guaranteed Bitrate (Mbps)	
	QOC-RRM [21]	LSTM-RRM
400	85	178
600	90	185
800	95	193
1000	99	200
1200	120	210
1400	130	228

Figure 15 and Table 14 show the outdoor guaranteed rate comparison between QOC-RRM [21] and LSTM-RRM. Here, the comparison is made by varying the building distance from 400 m to 1400 m. From the analysis, it can be seen that the LSTM-RRM achieves a higher outdoor guaranteed rate than the QOC-RRM [21]. For example, the outdoor guaranteed rate of the LSTM-RRM varies from 178 Mbps to 228 Mbps, whereas the outdoor guaranteed rate of the QOC-RRM [21] varies from 168 Mbps to 174 Mbps. Specifically, the outdoor guaranteed bitrate of LSTM-RRM for a building distance of 1400 m is improved up to 31.03% when compared to the QOC-RRM [21].

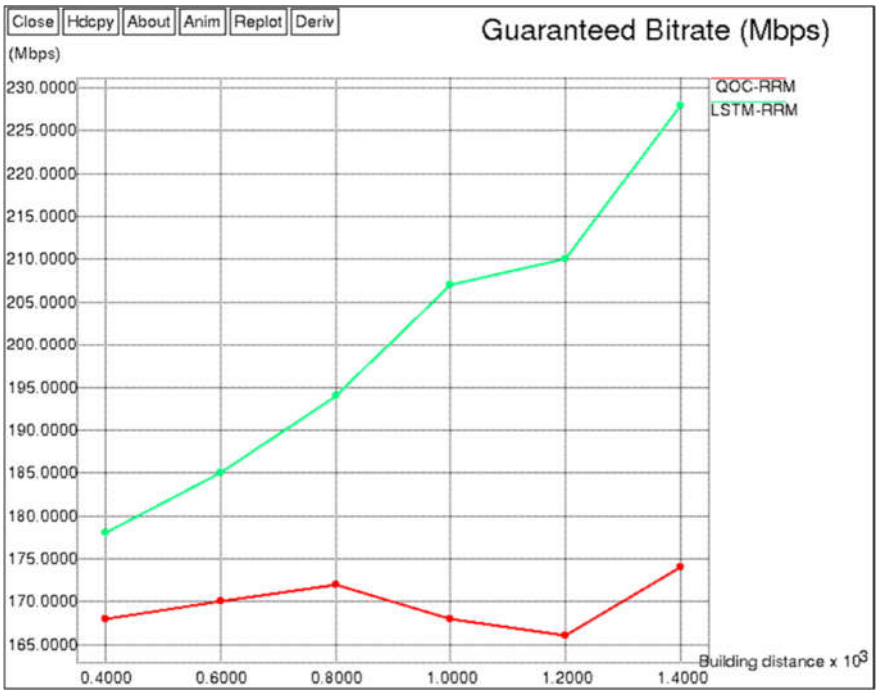

Figure 15. Comparison of outdoor guaranteed rate.

Table 14. Analysis of outdoor guaranteed rate for LSTM-RRM and QOC-RRM.

Building Distance (m)	Outdoor Guaranteed Bitrate (Mbps)	
	QOC-RRM [21]	LSTM-RRM
400	168	178
600	170	185
800	172	194
1000	168	207
1200	166	210
1400	174	228

From the analysis, it can be concluded that the LSTM-based RRM provides better performance than the DRRM [20], QOC-RRM [21], and EPAS [30], individually. The QOS parameters of the LSTM-based RRM are high due to its optimal bandwidth and power allocation to the user equipment of the 5G network. Moreover, the LSTM provides optimal results during the RRM because of the hyperparameters identified from GSO. Here, a queue-based RRM is used to minimize the traffic during data transmission. Moreover, the ISI caused in the network is reduced via guard level insertion in the data. Hence, the sum rate and guaranteed rate are increased while transmitting the data packets under burst errors.

5. Conclusions

In this paper, an LSTM-based RRM is proposed to allocate the optimum power and bandwidth to the desired UE based on the data rate. Here, the hyperparameters of the LSTM are identified using GSO, which further improves the performance of RRM. The request queue is considered in the 5G system to accomplish the priority-based resource allocation for the desired UEs. The priority-based RRM minimizes the traffic and avoids the unwanted resource allocation through the 5G environment. Moreover, the burst error and ISI in the 5G environment are minimized by using frequency interleaving and guard interval insertion. The LSTM-RRM method performs the power allocation in both the macro and micro cells of 5G environment. The performance of the LSTM-RRM method is improved in terms of throughput, outage percentages, and dual connectivity when compared to the DRRM, QOC-RRM, or EPAS. The indoor guaranteed rate of LSTM-RRM for a building distance of 1400 m is improved up to 75.38% when compared to the QOC-RRM.

Author Contributions: The paper investigation, resources, data curation, writing—original draft preparation, writing—review and editing, and visualization were done by K.R.B. and S.K. The paper conceptualization, software, validation, and formal analysis were done by K.M.V.G. and H.K.L. Methodology, supervision, project administration, and final approval of the version to be published were conducted by W.-C.L. and P.B.D. All authors have read and agreed to the published version of the manuscript.

Funding: This research received no external funding.

Institutional Review Board Statement: Not applicable.

Informed Consent Statement: Not applicable.

Data Availability Statement: Not applicable.

Conflicts of Interest: The authors declare no conflict of interest.

References

1. Condoluci, M.; Araniti, G.; Molinaro, A.; Iera, A. Multicast resource allocation enhanced by channel state feedbacks for multiple scalable video coding streams in LTE networks. *IEEE Trans. Veh. Technol.* **2015**, *65*, 2907–2921. [CrossRef]
2. De La Fuente, A.; Escudero-Garzás, J.J.; García-Armada, A. Radio resource allocation for multicast services based on multiple video layers. *IEEE Trans. Broadcast.* **2017**, *64*, 695–708. [CrossRef]
3. Pramudito, W.; Alsusa, E. A hybrid resource management technique for energy and QoS optimization in fractional frequency reuse based cellular networks. *IEEE Trans. Commun.* **2013**, *61*, 4948–4960. [CrossRef]
4. Li, Q.; Hu, R.Q.; Qian, Y.; Wu, G. Intracell cooperation and resource allocation in a heterogeneous network with relays. *IEEE Trans. Veh. Technol.* **2012**, *62*, 1770–1784. [CrossRef]
5. Wang, H.; Rosa, C.; Pedersen, K.I. Dual connectivity for LTE-advanced heterogeneous networks. *Wirel. Netw.* **2016**, *22*, 1315–1328. [CrossRef]
6. Soret, B.; Pedersen, K.I. Centralized and distributed solutions for fast muting adaptation in LTE-advanced HetNets. *IEEE Trans. Veh. Technol.* **2014**, *64*, 147–158. [CrossRef]
7. Belleschi, M.; Fodor, G.; Della Penda, D.; Pradini, A.; Johansson, M.; Abrardo, A. Benchmarking practical RRM algorithms for D2D communications in LTE advanced. *Wirel. Pers. Commun.* **2015**, *82*, 883–910. [CrossRef]
8. Naqvi, S.A.R.; Pervaiz, H.; Hassan, S.A.; Musavian, L.; Ni, Q.; Imran, M.A.; Ge, X.; Tafazolli, R. Energy-aware radio resource management in D2D-enabled multi-tier HetNets. *IEEE Access* **2018**, *6*, 16610–16622. [CrossRef]
9. Kaddour, F.Z.; Vivier, E.; Mroueh, L.; Pischella, M.; Martins, P. Green opportunistic and efficient resource block allocation algorithm for LTE uplink networks. *IEEE Trans. Veh. Technol.* **2014**, *64*, 4537–4550. [CrossRef]
10. Tiwana, M.I.; Tiwana, M.I. A novel framework of automated RRM for LTE son using data mining: Application to LTE mobility. *J. Netw. Syst. Manag.* **2014**, *22*, 235–258. [CrossRef]
11. Elgendy, O.A.; Ismail, M.H.; Elsayed, K.M. Radio resource management for LTE-A relay-enhanced cells with spatial reuse and max–min fairness. *Telecommun. Syst.* **2018**, *68*, 643–655. [CrossRef]
12. Tseliou, G.; Adelantado, F.; Verikoukis, C. Scalable RAN virtualization in multitenant LTE-A heterogeneous networks. *IEEE Trans. Veh. Technol.* **2015**, *65*, 6651–6664. [CrossRef]
13. Saddoud, A.; Doghri, W.; Charfi, E.; Fourati, L.C. 5G radio resource management approach for multi-traffic IoT communications. *Comput. Netw.* **2020**, *166*, 106936. [CrossRef]
14. Benzaid, C.; Taleb, T. AI-driven zero touch network and service management in 5G and beyond: Challenges and research directions. *IEEE Netw.* **2020**, *34*, 186–194. [CrossRef]

15. Jo, S.; Jong, C.; Pak, C.; Ri, H. Multi-agent deep reinforcement learning-based energy efficient power allocation in downlink MIMO-NOMA systems. *IET Commun.* **2021**, *15*, 1642–1654. [CrossRef]
16. Cai, T.; van de Beek, J.; Nasreddine, J.; Petrova, M.; Mähönen, P. A TD-LTE prototype system with modules for general-purpose cognitive resource management and radio-environmental mapping. *Int. J. Wirel. Inf. Netw.* **2011**, *18*, 131–145. [CrossRef]
17. Haddad, M.; Elayoubi, S.E.; Altman, E.; Altman, Z. A hybrid approach for radio resource management in heterogeneous cognitive networks. *IEEE J. Sel. Areas Commun.* **2011**, *29*, 831–842. [CrossRef]
18. Rostami, S.; Arshad, K.; Rapajic, P. Optimum radio resource management in carrier aggregation based LTE-advanced systems. *IEEE Trans. Veh. Technol.* **2017**, *67*, 580–589. [CrossRef]
19. Wang, H.; Rosa, C.; Pedersen, K.I. Radio resource management for uplink carrier aggregation in LTE-Advanced. *EURASIP J. Wirel. Commun. Netw.* **2015**, *1*, 121. [CrossRef]
20. Monteiro, V.F.; Sousa, D.A.; Maciel, T.F.; Cavalcanti, F.R.P.; e Silva, C.F.; Rodrigues, E.B. Distributed RRM for 5G multi-RAT multiconnectivity networks. *IEEE Syst. J.* **2018**, *13*, 192–203. [CrossRef]
21. Prasad, G.; Rukmini, M.S.S. Radio resource management strategy for mobile networks based on qos sensible confederation. *Test Eng. Manag.* **2020**, *83*, 1761–1769.
22. Pramudito, W.; Alsusa, E. Confederation based RRM with proportional fairness for soft frequency reuse LTE networks. *IEEE Trans. Wirel. Commun.* **2014**, *13*, 1703–1715. [CrossRef]
23. Ali, K.B.; Zarai, F.; Khdhir, R.; Obaidat, M.S.; Kamoun, L. QoS aware predictive radio resource management approach based on MIH protocol. *IEEE Syst. J.* **2018**, *12*, 1862–1873. [CrossRef]
24. Sande, M.M.; Hlophe, M.C.; Maharaj, B.T. Access and radio resource management for IAB networks using deep reinforcement learning. *IEEE Access* **2021**, *9*, 114218–114234. [CrossRef]
25. Pagin, M.; Zugno, T.; Polese, M.; Zorzi, M. Resource management for 5G NR integrated access and backhaul: A semi-centralized approach. *IEEE Trans. Wirel. Commun.* **2021**, *21*, 753–767. [CrossRef]
26. Zhao, G.; Li, Y.; Xu, C.; Han, Z.; Xing, Y.; Yu, S. Joint power control and channel allocation for interference mitigation based on reinforcement learning. *IEEE Access* **2019**, *7*, 177254–177265. [CrossRef]
27. Giannopoulos, A.; Spantideas, S.; Kapsalis, N.; Karkazis, P.; Trakadas, P. Deep reinforcement learning for energy-efficient multi-channel transmissions in 5G cognitive hetnets: Centralized, decentralized and transfer learning based solutions. *IEEE Access* **2021**, *9*, 129358–129374. [CrossRef]
28. Kaloxylos, A.; Gavras, A.; Camps Mur, D.; Ghoraishi, M.; Hrasnica, H. AI and ML—Enablers for beyond 5G networks. *Zenodo Tech. Rep.* **2020**, *1–145*. [CrossRef]
29. Sang, J.; Zhou, T.; Xu, T.; Jin, Y.; Zhu, Z. Deep learning based predictive power allocation for V2X communication. *IEEE Access* **2021**, *9*, 72881–72893. [CrossRef]
30. Hao, W.; Sun, G.; Zeng, M.; Chu, Z.; Zhu, Z.; Dobre, O.A.; Xiao, P. Robust design for intelligent reflecting surface-assisted MIMO-OFDMA terahertz IoT networks. *IEEE Internet Things J.* **2021**, *8*, 13052–13064. [CrossRef]
31. Javornik, T.; Švigelj, A.; Hrovat, A.; Mohorčič, M.; Alič, K. Distributed rem-assisted radio resource management in LTE-a networks. *Wirel. Pers. Commun.* **2017**, *92*, 107–126. [CrossRef]
32. Jacobsen, T.H.; Abreu, R.; Berardinelli, G.; Pedersen, K.I.; Kovács, I.Z.; Mogensen, P. Multi-cell reception for uplink grant-free ultra-reliable low-latency communications. *IEEE Access* **2019**, *7*, 80208–80218. [CrossRef]
33. Saleh, H.; Alharbi, A.; Alsamhi, S.H. OPCNN-FAKE: Optimized convolutional neural network for fake news detection. *IEEE Access* **2021**, *9*, 129471–129489. [CrossRef]